Available online at www.sciencedirect.com

ScienceDirect

International Journal of Mass Spectrometry 261 (2007) 208–217

International Journal of Mass Spectrometry

www.elsevier.com/locate/ijms

Vacuum-UV and electron dissociative ionisation studies of SF_5Cl

R.Y.L. Chim[a], P. Cicman[c,1], T.D. Märk[c], C.A. Mayhew[b], P. Scheier[c], R.P. Tuckett[a,*]

[a] School of Chemistry, University of Birmingham, Edgbaston, Birmingham B15 2TT, UK
[b] School of Physics and Astronomy, University of Birmingham, Edgbaston, Birmingham B15 2TT, UK
[c] Institut für Ionenphysik, Leopold Franzens Universitat, Technikerstrasse 25, A-6020 Innsbruck, Austria

Received 18 July 2006; received in revised form 7 September 2006; accepted 12 September 2006
Available online 20 October 2006

Abstract

A complementary study of the interaction of SF_5Cl in the gas phase with vacuum-UV photons and low-energy electrons from the onset of ionisation, ca. 12 eV, up to 20 eV is presented. The photon-induced experiments have used tunable vacuum-UV radiation from a synchrotron and threshold photoelectron photoion coincidence spectroscopy for product ion detection, the electron-induced experiments a trochoidal electron monochromator and a quadrupole mass spectrometer. The strengths and limitations of both experiments are contrasted, the main difference being the absence of state selectivity in the electron-induced study. The parent cation is not observed in either study, suggesting that its ground electronic state is repulsive following Franck–Condon vertical excitation. The fragment cations SF_5^+, SF_4Cl^+, SF_4^+ and SF_3^+ have been observed in both studies, with reasonable agreement in their threshold appearance energies. Using a variant of threshold photoelectron photoion coincidence spectroscopy applicable when the ground state of the parent cation is repulsive, the first dissociative ionisation energy of SF_5Cl is determined to be 12.3 ± 0.2 eV, leading to a value for the adiabatic ionisation energy for the SF_5 radical of 9.92 ± 0.28 eV. The electron-induced experiment is sensitive to ion-pair production, and onsets for F^+ and Cl^+ production have been observed which are only possible energetically if the accompanying fragments are the anions SF_4Cl^- and SF_5^-, respectively. A lower limit for the electron affinity of the SF_4Cl radical of 4.88 eV is determined, a value confirmed by ab initio calculations. The electron-induced experiment is very sensitive to gas impurities, and the effects of minute quantities of SF_4, FCl, Cl_2 and possibly SF_2 in the gas sample are observed.

Keywords: Photoionisation; Electron ionisation; Threshold photoelectron and coincidence spectroscopy; Appearance thresholds; SF_5Cl

1. Introduction

There have been a large number of investigations of the positive ion chemistry of sulfur hexafluoride, SF_6, e.g. [1–3], but relatively few of the derivative molecule sulfur chloropentafluoride, SF_5Cl. Recent interest in the chemistry of such molecules has come from the use of SF_6 in reactive plasmas for the etching of insulating and semiconducting layers [2]. In such environments, there is a large density of low-energy electrons causing both ionisation and fragmentation of the etchant gas, and it is important to understand the fundamental physics of how such molecules interact both with low-energy electrons and with vacuum-UV (VUV) photons whose energies cover the same range. In this paper we describe a complementary study of the interaction of SF_5Cl with low-energy electrons and VUV photons from the onset of ionisation, ca. 12 eV, up to 20 eV. The electron impact measurements were made in Innsbruck, Austria, the photon measurements at the Daresbury Synchrotron Radiation Source (SRS), UK. This paper forms a parallel study to the interaction and attachment of low-energy ($0 < E < 14$ eV) electrons with SF_5Cl in four European centres (Berlin, Birmingham, Kaiserslautern and Innsbruck) [4].

The structure of SF_5Cl in the gas phase has been established by microwave spectroscopy [5,6] and electron diffraction [7].

Abbreviations: AE, appearance energy; DIE, dissociative ionisation energy; EA, electron affinity; FWHM, full width at half maximum; HOMO, highest-occupied molecular orbital; KE, kinetic energy; KERD, kinetic energy release distribution; MP2, Möller Plesset 2; PIMS, photoionisation mass spectrometry; TDC, time-to-digital converter; TEM, trochoidal electron monochromator; TOF-MS, time-of-flight mass spectrometry; TPEPICO, threshold photoelectron photoion coinicdence; VUV, vacuum ultraviolet

[*] Corresponding author. Tel.: +44 121 414 4425; fax: +44 121 414 4403.
E-mail address: r.p.tuckett@bham.ac.uk (R.P. Tuckett).

[1] Present address: Department of Physics and Astronomy, University of Aarhus, DK-8000 Aarhus, Denmark.

1387-3806/$ – see front matter © 2006 Elsevier B.V. All rights reserved.
doi:10.1016/j.ijms.2006.09.025

The molecule has C_{4v} symmetry with an S–Cl bond length of 0.204 nm, four S–F equitorial bond lengths of 0.157 nm and one S–F axial bond length of 0.159 nm. All the XSY (X, Y = F or Cl) bond angles are very close to 90°. The fundamental vibrational frequencies of SF_5Cl which are infrared and Raman active have been observed in an argon matrix [8]. There has only been one He I and He II photoelectron study of this molecule [9], and the relative ordering of the valence molecular orbitals has been calculated using the self-consistent discrete variational Xα method [10]. There have been no photoelectron studies under threshold conditions. The positive fragment ions formed by electron ionisation and photoionisation mass spectrometry (PIMS) have been studied in the range 12–20 eV [11,12], but no spectra have been recorded under coincidence conditions. It has not therefore been possible to correlate appearance of certain fragment cations with dissociation of a particular electronic state of SF_5Cl^+. Inner-shell photoabsorption has been studied in the range 160–210 eV [13] and in the sulfur and chlorine K-edge region of 2400–3100 eV [14]. There have been two earlier studies of the fragment anions formed from low-energy ($E < 10$ eV) electron attachment to SF_5Cl [11,15], in addition to the recent study of Braun et al. mentioned above [4]. There has been no study to date of ion-pair production following VUV photoexcitation of SF_5Cl (e.g., $SF_5Cl + h\nu \rightarrow SF_5^+ + Cl^-$ or $SF_4Cl^+ + F^-$), parallel to that reported by Mitsuke et al. for SF_6 [16]. The kinetics of low-energy electron attachment, of anion, and of cation reactions with SF_5Cl has been studied in recent years by Mayhew and co-workers [17–19]. Finally, the structure and stability of fragments of SF_5Cl and SF_5Cl^- have been investigated by density functional methods [20].

In this paper, we report the first observation of threshold photoelectron and threshold photoelectron photoion coincidence (TPEPICO) spectra of SF_5Cl in the range 12–20 eV. Appearance energies and ion yields over this photon range are determined. Using a method developed by us to measure the first dissociative ionisation energy (DIE) of molecules whose ground electronic state of the parent cation is repulsive [21], we have confirmed the literature value for the enthalpy of formation of SF_5^+ and hence the adiabatic ionisation energy of the SF_5 radical [21,22]. We have also measured the mean translational kinetic energy release, $\langle KE \rangle_T$, from fragmentation of electronic states of SF_5Cl^+ with defined energy into either $SF_5^+ + Cl$ or $SF_4Cl^+ + F$, via a single bond cleavage. The weakness of the signals from the TPEPICO data has meant that some appearance energies are poorly determined. To confirm these data, we have measured threshold energies using non-state-selective electron ionisation. In Innsbruck, therefore, we have measured the fragment cations produced from low-energy electron impact excitation ($10 < E < 25$ eV) of SF_5Cl to compare appearance energies. Since the cations are now not measured in coincidence with an associated photoelectron, this technique is also sensitive to ion-pair production and we have observed two such channels ($SF_5Cl + e^- \rightarrow Cl^+ + SF_5^- + e^-$ and $F^+ + SF_4Cl^- + e^-$). Thus, we have been able to confirm the literature value for the electron affinity (EA) of SF_5, and report the first value for the EA of the SF_4Cl radical.

2. Experimental

The apparatus used for the photoionisation study has been described in detail previously [23]. Experiments were performed at the Daresbury SRS on station 3.1 using a 1 m focal length Seya monochromator, range ca. 8–40 eV, with an optimum resolution of 0.08 nm. Although fitted with two gratings, the experiments only used the lower-energy grating with a range ca. 8–22 eV. The synchrotron radiation is coupled into the interaction region, via a capillary and the flux is monitored by a photomultiplier tube through a sodium salicylate window, allowing for flux normalisation of spectra where the monochromator is scanned. Threshold photoelectrons and fragment cations are extracted in opposite directions by an electric field of 20 V cm^{-1}. The electrons are detected in a threshold analyser with resolution ca. 10 meV, the ions in a linear time-of-flight (TOF) mass spectrometer with a resolution $m/\Delta m$ of ca. 200. The signals are detected by a channeltron and a pair of microchannel plates, respectively. The raw data pulses are discriminated and pass to a time-to-digital converter (TDC). The electrons provide a start to the TOF detection window and the ions provide a stop, allowing signals from the same ionisation event to be detected in coincidence. Spectra are measured as a function of photon energy, where the data record as a three-dimensional map of coincidence count versus ion TOF versus photon energy. These spectra can yield either the TOF mass spectrum (TOF-MS) at any photon energy or the yield of any fragment ion as a function of energy. Extraction of product branching ratios as a function of photon energy is facile, and in addition the threshold photoelectron spectrum is recorded simultaneously.

In a high resolution variant of this experiment [21], in order to determine the first DIE of SF_5Cl (Section 3) the TOF-MS of SF_5^+ was recorded with high time resolution of the TDC over the limited range 12.0–14.3 eV, encompassing only the Franck–Condon region of the ground state of SF_5Cl^+. It was then possible to determine the value of $\langle KE \rangle_T$ into $SF_5^+ + Cl$ as a function of $h\nu$ over this range of energies. In more conventional experiments at a fixed photon energy, the kinetic energy release distribution (KERD) and $\langle KE \rangle_T$ were determined from the TOF mass spectra recorded for both SF_5^+ and SF_4Cl^+, corresponding to breaking a single S–Cl or S–F bond, respectively. The ratio of $\langle KE \rangle_T$ to the energy available shows what fraction, $\langle f \rangle_T$, is channelled into translational motion of the two fragments. The value of $\langle f \rangle_T$ can be compared to that from statistical and impulsive models to indicate the mechanism of dissociation; full details can be found elsewhere [24].

The apparatus used for the electron impact excitation experiments has also been described in detail elsewhere [25]. It comprises a trochoidal electron monochromator (TEM), an effusive molecular beam, and a quadrupole mass spectrometer with pulse counting for detection of product ions. The quadrupole can detect either cations or anions. In the TEM, the electrons are monochromatised using crossed electric and magnetic fields, and the electrons drift perpendicular to both fields to an aperture that is horizontally displaced with respect to the incident beam. The resolution of the electron beam under optimum conditions is 30 meV FWHM with an electron current of ca. 0.5 nA.

In these experiments, for flux reasons the electron resolution is degraded to ca. 200 meV, and the current is two orders of magnitude greater. SF_5Cl is admitted as an effusive beam to the interaction region from a 20 μm nozzle backed by ca. 10 mbar of sample, and crosses the tunable electron beam orthogonally. Cations are extracted with as low an extraction field as possible to minimise mass discrimination effects, and pass through the quadrupole mass filter, resolution set at ca. 1.5 u, which is mounted on the axis of the molecular beam. Signals were normalised to any variations of sample pressure in the interaction region and the electron current. The electron energy scale was calibrated against the appearance energy of rare gas ions, e.g., the Ar^+ $^2P_{3/2}$ threshold at 15.759 eV [26], with an estimated accuracy of better than 20 meV.

Different samples of SF_5Cl were used at Daresbury and Innsbruck, but both were provided from Apollo Scientific Ltd. with a stated purity of 97%. No further purification was carried out in either experiment. The results of the Innsbruck study (Section 4.2) showed that SF_4, FCl and Cl_2 were significant impurity species. The presence of SF_4 and FCl is not surprising because these molecules are used to synthesise SF_5Cl. In their electron attachment study of SF_5Cl, Fenzlaff et al. [15] synthesised their own sample, and commented that SF_2O was present in small amounts resulting from hydrolysis of SF_4. A 70 eV electron impact mass spectrum recorded at Innsbruck did indeed show the presence of hydrolysis impurities, with very weak peaks at 83, 86 and 105 u assigned to $SFO_2{}^+$, SF_2O^+ and SF_3O^+, respectively. The presence of such impurities is not as significant in the Daresbury experiments because the ions are detected in coincidence with energy-analysed photoelectrons.

3. Data analysis and energetics

The three-dimensional coincidence spectra were analysed in the usual way to give appearance energies (AE) of the fragment ions, ion yield curves and branching ratios [23]. The AE_{298} values are listed in column 2 of Table 1. They are determined from the first observation of signal above the background noise. At the resolution (0.3 nm) and step size used in these experiments, this is equivalent to extrapolation of the linear portion of the ion yield to zero signal, and more sophisticated fitting procedures for the threshold region are not appropriate [27]. For the major fragment ions, defined as those formed by a single bond cleavage, the AE_{298} values can be converted into an upper limit of $\Delta_r H^o_{298}$ for the corresponding unimolecular reaction (column 1) using the procedure of Traeger and McLoughlin [28], and are given in column 4 (denoted $\Delta_r H^o_{298,\text{exp}}$). The upper limit arises due to the possible presence of an exit-channel barrier and/or a kinetic shift; if both are zero, the conversion is exact. This procedure was developed for interpretation of photoionisation

Table 1

Thermochemistry of observed dissociative ionisation pathways of SF_5Cl at 298 K

Dissociation pathway	AE_{298}[a] (eV)	EI threshold at 298 K[b] (eV)	$\Delta_r H^o_{298,\text{exp}}$[c] (eV)	$\Delta_r H^o_{298,\text{calc}}$[d] (eV)	$AE_{298,\text{ calc}}$[e] (eV)
Major[f] products of SF_5Cl (−1039)[g]					
$SF_5{}^+$ (+29) + Cl (+121) + e^-	12.3 (2)	12.65 (2)	12.47 (20)	12.32	12.15
SF_4Cl^+ (+327)[h] + F (+79) + e^-	14.8 (2)	15.38 (9)	14.98 (20)	≤14.98[h]	≤14.80
Cl^+ (+1372) + $SF_5{}^-$ (−1282)	–	12.85 (5)	–	11.70	11.53
F^+ (+1760) + SF_4Cl^- (≤−1232)	–	16.08 (6)	–	≤16.24	≤16.06
Minor[i] products of SF_5Cl (−1039)					
$SF_4{}^+$ (+365) + FCl (−50) + e^-	16.2 (2)	16.05 (5)		14.03	
$SF_4{}^+$ (+365) + F (+79) + Cl (+121) + e^-				16.62	
$SF_3{}^+$ (+286) + FCl (−50) + F (+79) + e^-	16.8 (4)	16.5(1)		14.03	
$SF_3{}^+$ (+286) + F_2 (0) + Cl (+121) + e^-				14.99	
$SF_3{}^+$ (+286) + 2F (+158) + Cl (+121) + e^-				16.62	
Impurity peaks[j]					
$SF_4{}^+$ (108 u) (from SF_4)		12.0 (1.9)			
$SF_3{}^+$ (89 u) (from SF_4)		12.0 (6)			
$SF_2{}^+$ (70 u) (from SF_2)		10.39 (16)			
SF^+ (51 u) (from SF_2)		12.87 (25)			
$Cl_2{}^+$ (72 u) (from Cl_2)		11.26 (26)			
FCl^+ (54 u) (from FCl)		12.17 (24)			

[a] Experimental appearance energy from photoionisation experiment, measured from first onset of signal above noise.

[b] Experimental threshold from electron ionisation experiment, determined from fit to analytical function described in Section 3.

[c] Experimental enthalpy of reaction, derived from AE_{298} using method of Traeger and McLoughlin [28].

[d] Calculated enthalpy of reaction, given by enthalpy of formation of products minus that of reactants.

[e] Calculated appearance energy at 298 K, derived from $\Delta_r H^o_{298,\text{calc}}$ using the method of Traeger and McLoughlin [28].

[f] Major products are defined as fragment cations caused by breaking a single bond.

[g] Literature values for $\Delta_f H^o_{298}$ (in kJ mol^{-1}) are given in brackets in column 1, taken from [26,31,33]. Exceptions are $\Delta_f H^o_{298}(SF_5) = -915$ [22], $\Delta_f H^o_{298}(SF_5^+) = +29$ [21], $\Delta_f H^o_{298}(SF_5^-) = -1282$ [15,22], $\Delta_f H^o_{298}(SF_4Cl) = -761$ [19], $\Delta_f H^o_{298}(SF_4Cl^+) = +327$ [19,this work], $\Delta_f H^o_{298}(SF_4Cl^-) \leq -1232$ [19,this work], $\Delta_f H^o_{298}(SF_4^+) = +365$ [22,31] and $\Delta_f H^o_{298}(SF_3^+) = +286$ [22,31], all in units of kJ mol^{-1}.

[h] In the absence of a value for the ionisation energy of SF_4Cl, it is assumed that SF_4Cl^+ turns on at its thermochemical threshold. Thus, this value for $\Delta_f H^o_{298}(SF_4Cl^+)$ is an upper limit.

[i] Minor products are defined as fragment cations caused by breaking more than one bond.

[j] Impurity peaks are derived from neutral molecules that should not be present in the SF_5Cl sample.

yields rather than state-selected TPEPICO yields, but we have shown that the procedure is equally valid for both experiments [29,30]. For the vibrational frequencies of SF_5^+ and SF_4Cl^+ needed for these conversions, values for the isoelectronic neutral molecules PF_5 and PF_4Cl were used [31,32]; the differences of the vibrational frequencies due to a change in reduced mass of the sulfur and phosphorus analogues make negligible difference to these conversions. The predicted enthalpies of reaction at 298 K, $\Delta_r H^o_{298,\mathrm{calc}}$ are listed in column 5, using enthalpies of formation at 298 K of reactants or products mostly taken from standard sources [26,31,33]. Exceptions are given as a footnote to Table 1. The corresponding lower values of $AE_{298,\,\mathrm{calc}}$, determined as above [28], are given in column 6. Comparison of AE_{298} for each minor ion with $\Delta_r H^o_{298,\mathrm{calc}}$ allows the neutral partner(s) that form with each fragment ion to be elucidated.

Since the behaviour of atoms and small molecules just above threshold differs for electron and photon excitation, the electron ionisation data were analysed differently to establish thresholds for fragment ion production (defined E_o, column 3 of Table 1). Ignoring instrumental effects, with electron ionisation the cross-section for molecules at energy $E > E_o$ is proportional to $(E - E_o)^x$, where x typically takes values between 1.2 and 2.0 [34]; with photoionisation, the cross-section shows a step function at threshold modulated by Franck–Condon factors. Thus, each electron ionisation function in the threshold region was fitted by a non-linear least squares fit to:

$$\sigma(E) = b + c(E - E_o)^x, \quad \text{for } E > E_o \tag{1}$$

For $E \leq E_o$, the value of the cross-section is constrained to the background noise level, b. If the excitation function involves two thresholds, then an extra term $d(E - E_o)^y$ is added to the function for $\sigma(E)$ when $E > E_o$. Data are fitted from approximately 2 eV below to 2 eV above threshold. Fits therefore involve four (for a single threshold) or seven (for a double threshold) parameters. Whilst being somewhat subjective, the appearance of the fitted curve together with the value of χ^2 allow sensible fits to be made to the data.

We now describe how the data for the variation of $\langle KE \rangle_T$ with photon energy is analysed. This technique can be applied to determine the first DIE of molecules with ground electronic states of the parent cation which are repulsive in the Franck–Condon region (e.g., CF_4, SF_6 and CF_3SF_5 [21]). It is equally applicable for SF_5Cl, where the first DIE is defined to be the threshold energy for $SF_5Cl \rightarrow SF_5^+ + Cl + e^-$. The translational KE released into the $SF_5^+ + Cl$ fragments is measured by coincidence spectroscopy as a function of photon energy, $h\nu$, over the Franck–Condon region of the ground state of SF_5Cl^+. $\langle KE \rangle_T$ will correspond to some fraction of the available energy, E_{avail}, where

$$\begin{aligned} E_{\mathrm{avail}} &= h\nu + (\text{thermal energy of } SF_5Cl \text{ at temperature } T) \\ &\quad - \mathrm{DIE}(SF_5Cl) \end{aligned} \tag{2}$$

The value of $\langle f \rangle_T$ is governed by the dynamics of the decay mechanism [23], and cannot unambiguously be determined from a measurement at one value of $h\nu$. By measuring $\langle KE \rangle_T$ continuously as a function of $h\nu$, however, and assuming that $\langle f \rangle_T$ is independent of energy, $\langle KE \rangle_T$ increases at a constant rate with $h\nu$. Extrapolation to a KE release of zero gives an intercept on the photon energy axis which equals the first DIE of SF_5Cl. The method of obtaining $\langle KE \rangle_T$ from such spectra is described below. If the dissociation mechanism is purely impulsive [35], meaning dissociation occurs on a timescale much faster than other processes such as intramolecular vibrational redistribution, then the slope of the graph is determined solely by kinematics, and given by the ratio of two reduced masses, $\mu_{S,Cl}/\mu_{SF_5,Cl}$. For dissociation of SF_5Cl to $SF_5^+ + Cl$, the value of 0.61 is then the reduced mass of the two atoms whose bond is broken divided by the reduced mass of the two product fragments.

Fixed-energy TPEPICO-TOF mass spectra were recorded with the optimal TOF resolution of the TDC, 8 ns, for SF_5^+ at photon energies of 13.05, 15.12, 15.90 and 16.87 eV, corresponding approximately to excitation of the $\tilde{X}\ ^2E$, $\tilde{B}\ ^2A_2$, $\tilde{C}\ ^2E$, $\tilde{D}\ ^2E$ states of SF_5Cl^+, and for SF_4Cl^+ at energies of 15.90 and 16.87 eV. $\langle KE \rangle_T$ values were obtained using a method described elsewhere [36,37]. Briefly, for each TPEPICO-TOFMS spectrum a small set of peaks, each with a discrete energy release ε_t, is computed and assigned a probability. The discrete energies are given by $\varepsilon_t(n) = (2n-1)^2 \Delta E$, where $n = 1$, 2, 3, 4, ... ΔE depends on the statistical quality of the data; the higher the signal-to-noise ratio, the lower ΔE and the higher n can be set to obtain the best fit. Each computed peak in the kinetic energy release distribution spans the range $4(n-1)^2 \Delta E$ to $4n^2 \Delta E$, centred at $\varepsilon_t(n) + \Delta E$. The reduced probability of each discrete energy, $P(\varepsilon_t)$, is determined by minimising the least-squared errors between the simulated and experimental TOF peak. From the basis set of ε_t and $P(\varepsilon_t)$, $\langle KE \rangle_T$ is easily determined. The latest analysis programme can accommodate a range of isotopes in the daughter ion [37], and measurements of the SF_4Cl^+ spectra incorporated the ^{35}Cl:^{37}Cl isotope splitting in the statistical ratio of 3:1. In the experiment to determine the DIE of SF_5Cl, 64 TOF mass spectra need to be analysed simultaneously. The procedure is then simplified by constraining n to one and only varying ΔE. We have confirmed for a few energy channels that this mean value of the energy release is indeed very similar to the value of $\langle KE \rangle_T$ obtained from the full KERD.

4. Results

4.1. Photon excitation experiments

The threshold photoelectron spectrum of SF_5Cl was measured from 12 to 21 eV (Fig. 1) with a constant wavelength resolution of 0.3 nm, corresponding to 0.03 eV at 12 eV, 0.11 eV at 21 eV. The spectral resolution is determined by the monochromator in the beamline, and not the electron analyser. No vibrational structure is resolved. The onset of ionisation, defined as the energy at which signal is first observed above the background noise level, is 12.24 ± 0.03 eV. Peaks are observed at 13.02, 15.66, 16.69, 18.04 and 19.17 eV, corresponding to the $\tilde{X}$, $(\tilde{A}/\tilde{B}/\tilde{C})$, $\tilde{D}$, $\tilde{E}$ and $\tilde{F}$ states of SF_5Cl^+. There is reasonable agreement with the energies of these states from the He I data of DeKock et al. [9], although this earlier work was able to resolve the three peaks between 14.8 and 15.9 eV corresponding to

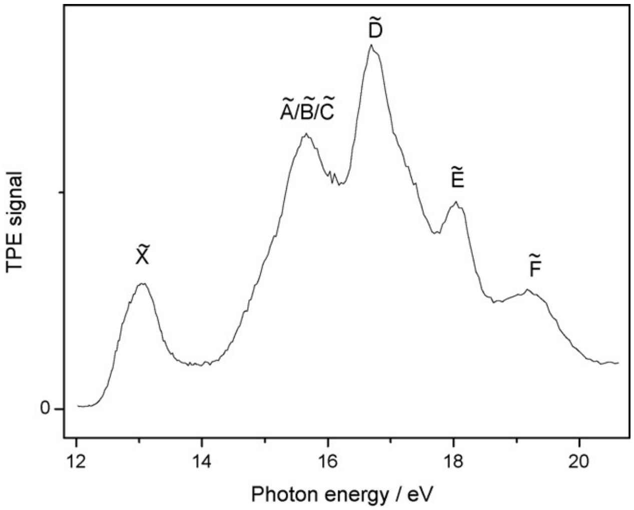

Fig. 1. Flux-normalised threshold photoelectron spectrum of SF_5Cl recorded at a resolution of 0.3 nm. The $\tilde{X}$, $\tilde{A}$, $\tilde{B}$, etc., labels refer to the ground state, first excited state, second excited state, etc., of the parent cation.

ionisation to the $\tilde{A}$, $\tilde{B}$, and $\tilde{C}$ states. Using an orbital numbering scheme that ignores core orbitals, the $\tilde{X}$ state of SF_5Cl^+ corresponds to electron removal from the 6e Cl 3pπ doubly-degenerate lone pair orbital [9,10], which correlates with two components of the $1t_{1g}$ triply-degenerate highest-occupied molecular orbital (HOMO) of SF_6; it therefore has term symbol ^2E in C_{4v} symmetry. Both sets of calculations performed on the MOs of SF_5Cl agree that the $\tilde{A}$, $\tilde{B}$, and $\tilde{C}$ states of SF_5Cl^+ have term symbols $^2A_1$, $^2A_2$ and ^2E, correlating with $3t_{1u}$ and one component of the $1t_{1g}$ HOMO of SF_6 [9,10]. The peaks at 16.69 and 18.04 eV incorporate ionisation from the 4e, $3b_1$, $6a_1$ and $2b_1$ orbitals of SF_5Cl, which correlate with the $1t_{2u}$ and $2e_g$ orbitals in SF_6. Calculations performed by us using Gaussian 03 at the MP2 level of theory with a 6-311-G + (d,p) basis set have shown that the (HOMO-1), (HOMO-2) and (HOMO-3) orbitals of SF_5Cl can approximately be described as S–$F_{\text{equitorial}}$ bonding, $F_{\text{equitorial}}$ 2pπ lone pair, and F_{axial} 2pπ lone pair with some $F_{\text{equitorial}}$–Cl overlap, respectively. The (HOMO-4), (HOMO-5) and (HOMO-6) orbitals, from which electron removal leads to production of the $\tilde{D}$ $^2A_1$, $\tilde{E}$ ^2E and $\tilde{F}$ $^2B_1$ states of SF_5Cl^+, have character S–$F_{\text{equitorial}}$, F_{axial} 2pπ lone pair with partial S–$F_{\text{equitorial}}$ bonding, and $F_{\text{equitorial}}$ 2pπ lone pair, respectively.

It is also instructive to compare the relative intensities of peaks recorded under threshold (i.e., resonant) and non-resonant conditions. Whilst electrons only arising from *direct* ionisation events are likely to be recorded in the He I spectrum, under threshold conditions electrons arising from autoionisation processes (i.e., $SF_5Cl + h\nu \rightarrow SF_5Cl^* \rightarrow SF_5Cl^+ + e^-$) will also be detected. The relative intensities of the bands are significantly different under the two conditions. In the threshold spectrum (Fig. 1), the relative intensity of the $\tilde{X}$-state band is anomalously low, whilst that of the unresolved ($\tilde{A}/\tilde{B}/\tilde{C}$) states is high. The $\tilde{X}$ and $\tilde{D}$ states at 12.87 and 16.72 eV dominate the He I spectrum [9], whilst this influence is not apparent in the threshold spectrum due to the much higher intensity of the ($\tilde{A}/\tilde{B}/\tilde{C}$) states. We conclude that significant autoionisation processes are occurring between ca. 15 and 17 eV under the conditions where electrons with zero energy are collected.

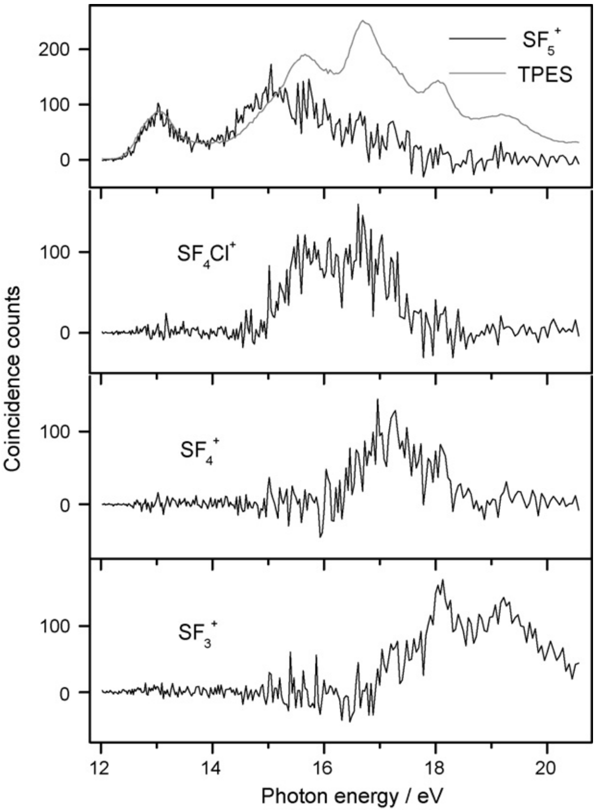

Fig. 2. Coincidence yield of the fragment ions SF_5^+, SF_4Cl^+, SF_4^+ and SF_3^+ from photoionisation of SF_5Cl, recorded at a resolution of 0.3 nm. The threshold photoelectron spectrum of SF_5Cl, not shown to scale, is shown with the SF_5^+ yield.

The scanning-energy TPEPICO spectrum of SF_5Cl was recorded from 12 to 26 eV with an optical resolution of 0.3 nm and an ion TOF resolution of 64 ns. Four fragment ions are observed; SF_5^+, SF_4Cl^+, SF_4^+ and SF_3^+. The parent ion is not observed. This is expected from thermochemical considerations, as the calculated energy of the $SF_5^+ + Cl + e^-$ dissociation channel, 12.15 eV, lies below the onset of ionisation of SF_5Cl. Therefore, the ground state of SF_5Cl^+ is repulsive in the Franck–Condon region along the S–Cl coordinate. The ion yields obtained from the spectrum are shown in Fig. 2, and AE_{298} values are given in column 2 of Table 1. Over the Franck–Condon region of the first photoelectron band, the SF_5^+ signal, onset 12.3 ± 0.2 eV, and the threshold photoelectron signal show a very similar variation with photon energy. The $\tilde{X}$ state of SF_5Cl^+ therefore dissociates exclusively to $SF_5^+ + Cl$. This is expected if ionisation from the HOMO of SF_5Cl removes an electron from a Cl 3pπ orbital and weakens the S–Cl bond, leading to prompt S–Cl bond dissociation before the cation charge redistributes over the molecule. Above ca. 15 eV, there is no obvious correlation between the SF_5^+ yield and the threshold electron signal. The yield of SF_4Cl^+, however, threshold 14.8 ± 0.2 eV, seems to mirror the electron signal over the energies of the ($\tilde{A}/\tilde{B}/\tilde{C}$) and $\tilde{D}$ states of SF_5Cl^+, ca. 15–18 eV. This is also expected if dissociation occurs on a more rapid timescale than intramolecular vibrational redistribution, since the character of the (HOMO-1) through (HOMO-4) orbitals is dominated by electron density between the S atom and the four equitorial F atoms. There is also some weak correlation between the SF_4^+ and SF_3^+ yields (thresholds observed at 16.2 ± 0.2 and 16.8 ± 0.4 eV, respectively) with the $\tilde{D}$ and $\tilde{E}$, and $\tilde{E}$ and $\tilde{F}$ states of SF_5Cl^+, respectively. SF_4^+ and SF_3^+ also have very weak secondary thresholds at 14.8 ± 0.2 and 15.0 ± 0.4 eV, respectively, energies significantly lower than the AE_{298} values of the main thresholds. The onset for formation of SF_4^+ lies close to the thermochemical threshold if atoms F + Cl form with this ion (Table 1), but ca. 2 eV above threshold if FCl is the neutral partner. Likewise, the onset for formation of SF_3^+ lies very close to the thermochemical threshold for production of this ion with F + F + Cl atoms, but 2–3 eV above threshold if a molecular neutral (F_2 or FCl) is formed. These data suggest that SF_4^+ forms from secondary and sequential dissociation of SF_5^+ of SF_4Cl^+, and SF_3^+ from secondary dissociation of SF_4^+. We should note, however, that formation of a molecular diatomic neutral is almost certain to involve an exit-channel barrier, so the experimental energetics cannot rule out the possibility of SF_4^+ and SF_3^+ forming from direct dissociation of SF_5Cl^+, via a constrained transition state. The AE values of the four ions observed in this study agree reasonably well with data from the PIMS study (SF_5^+ 12.32 eV, SF_4^+ 14.76 eV, SF_3^+ 15.87 eV, SF_3^+ 16.2 eV) [12]. The apparent observation of SCl^+ in this latter study has since been attributed to an impurity in the gas sample.[2]

The scanning-energy TPEPICO spectrum of the SF_5^+ fragment only was also recorded as a much higher TOF resolution of 16 ns over the limited energy range of 12.0–14.2 eV, encompassing the $\tilde{X}\,^2E$ state of SF_5Cl^+. This state dissociates exclusively to SF_5^+ + Cl. The theory underlying this experiment was described in Section 3. Fig. 3a shows the mean kinetic energy release, determined by the simplified method also described in Section 3, as a function of energy, whilst Fig. 3b shows the threshold photoelectron spectrum over this limited range of energies. Within experimental error, the lowest-energy data points that describe the rising edge of the $\tilde{X}$ state Franck–Condon region fit to a straight line with gradient 0.16 ± 0.03, but we note that this value is significantly less than the predicted value of 0.61 for this impulsive mechanism. Extrapolation to zero kinetic energy yields the first DIE of SF_5Cl to be 12.3 ± 0.2 eV. Using literature values for the 0 K enthalpies of formation of SF_5Cl and Cl [31], $\Delta_f H_0^o(SF_5^+)$ is determined to be $42 \pm 20\,\mathrm{kJ\,mol^{-1}}$, leading to an adiabatic IE (SF_5) of 9.92 ± 0.28 eV. The former value is in reasonable agreement with the value obtained from the dissociative photoionisation reaction $SF_6 + h\nu \rightarrow SF_5^+ + F + e^-$, $29 \pm 10\,\mathrm{kJ\,mol^{-1}}$ [21], and the value recommended by Fisher et al. from guided ion beam spectroscopy of $11 \pm 18\,\mathrm{kJ\,mol^{-1}}$ [22]. A value of the slope which is significantly less than the impulsive prediction was also observed for the three dissociative photoionisation reactions $XF_6 + h\nu \rightarrow XF_5^+ + F + e^-$ (X = S, Se or Te) [21,38], but the slope has the 'correct' value for the two reactions $CF_3X + h\nu \rightarrow CF_3^+ + F + e^-$ (X = F or SF_5) [21]. The pure impulsive model, where the slope should be determined solely by kinematics as the ratio of two reduced masses (Section 3), does not depend on the geometry of the fragment ion or the neutral parent molecule [35]. However, there is still uncertainty in the structure of SF_5^+ [39], and we note that this is not the case for CF_3^+. (Becker et al. [39] calculate two structures for SF_5^+ with very similar energies. The trigonal bipyramidal (D_{3h}) structure, although calculated to be the isomer with lower-energy, would need significant internal re-arrangement to occur following cleavage of the S–Cl bond, whereas the square pyramidal (C_{4v}) isomer lying 0.22 eV higher in energy would not.) The other difference between these two dissociation groups is that the SF_5^+-containing ions dissociate further to SF_4^+ (+F) and SF_3^+ (+2F or F_2) for relatively small amounts of extra photon energy, whereas this is not observed for the CF_3^+-containing ions.

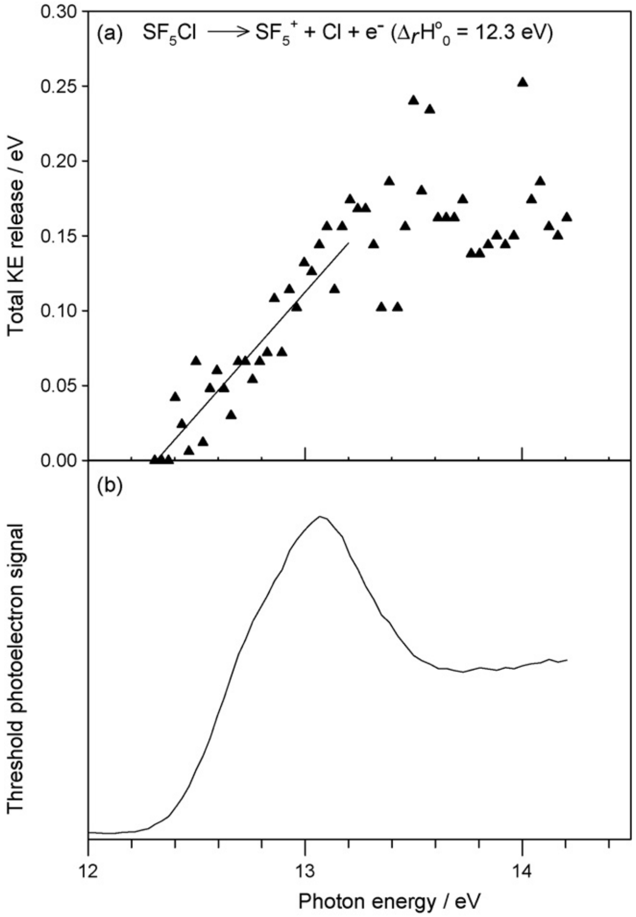

Fig. 3. (a) Mean total kinetic energy released in the reaction $SF_5Cl + h\nu \rightarrow SF_5^+ + Cl + e^-$ for photon energies in the range 12.0–14.2 eV. A linear extrapolation to zero kinetic energy gives the first dissociative ionisation energy of SF_5Cl, 12.3 ± 0.2 eV. The error in each value of the kinetic energy release is ca. 20%. (b) Threshold photoelectron spectrum of SF_5Cl over the same range of energies.

TPEPICO-TOF mass spectra were also recorded for SF_5^+ and SF_4Cl^+ at fixed photon energies corresponding to peaks in the threshold photoelectron spectrum. The results for $\langle KE \rangle_T$ and $\langle f \rangle_{T,\,expt}$ are shown in Table 2, as well as theoretical values for $\langle f \rangle_T$

---

[2] H.W. Jochims, private communication.

Table 2
Total mean translational kinetic energy release, $\langle KE \rangle_T$, for the two-body fragmentation of valence electronic states of SF_5Cl^+

Electronic state of parent ion		Daughter ion	$h\nu$ (eV)	E_{avail}[a] (eV)	$\langle KE \rangle_T$ (eV)	$\langle f \rangle_{T,\ expt}$[b]	$\langle f \rangle_T$[c] statistical	$\langle f \rangle_T$[d] impulsive
SF_5Cl^+	$\tilde{X}\ ^2E$	SF_5^+	13.05	1.03	0.26	0.25[e]	0.06	0.61
	$\tilde{B}\ ^2A_2$	SF_5^+	15.12	3.10	1.23	0.40	0.06	0.61
	$\tilde{C}\ ^2E$	SF_5^+	15.90	3.88	0.64	0.16	0.06	0.61
	$\tilde{D}\ ^2E$	SF_5^+	16.87	4.85	1.37	0.28	0.06	0.61
SF_5Cl^+	$\tilde{C}\ ^2E$	SF_4Cl^+	15.90	1.23[f]	1.14	0.93	0.06	0.71
	$\tilde{D}\ ^2E$	SF_4Cl^+	16.87	2.20[f]	1.35	0.61	0.06	0.71

[a] $E_{avail} = h\nu +$ thermal energy of SF_5Cl at 298 K (0.13 eV) − $AE_{298,\ calc}$. The vibrational frequencies for SF_5Cl are taken from Chase [31].

[b] $\langle f \rangle_T = \langle KE \rangle_T / E_{avail}$.

[c] Klots [40].

[d] Busch and Wilson [35].

[e] The signal-to-noise ratio of this spectrum is poor, and may explain why this value of $\langle f \rangle_T$ is significantly different from the value of 0.16 ± 0.03 obtained from a range of energies encompassing the $\tilde{X}$-state Franck–Condon region (Section 4.1).

[f] E_{avail} has been calculated assuming that SF_4Cl^+ turns on at its thermochemical threshold.

assuming statistical and pure impulsive limits for the dissociation mechanism. A full description of the statistical mechanism, and how $\langle KE \rangle_T$ is expected to vary with excess energy above threshold, has been given by Klots [40]. There appears to be no pattern in the $\langle f \rangle_T$ values for SF_5^+/SF_5Cl as $h\nu$ increases. Specifically, the full width at half maximum of the TPEPICO-TOF spectrum at 16.87 eV exceeds that at 15.12 eV, which exceeds that at 15.90 eV which itself is greater than that at 13.05 eV. The $\langle f \rangle_T$ value at 15.12 eV, dissociation approximately from the $\tilde{B}\ ^2A_2$ state of SF_5Cl^+, has the greatest value, 0.40. In measurements on other similar-sized ions [24], $\langle f \rangle_T$ often decreases as $h\nu$ increases, reflecting the larger density of vibronic states with increasing energy and hence the greater likelihood of statistical behaviour. This does not appear to be the case with SF_5Cl, and suggests that excited electronic states of SF_5Cl^+ show significant isolated-state behaviour. For SF_4Cl^+/SF_5Cl, the data suggest possible problems with the calculation of E_{avail}. The $\langle f \rangle_T$ value at 15.90 eV lies outside the statistical and impulsive limits. It should be noted that since the ionisation energy of the SF_4Cl radical is unknown, it has been assumed that the appearance energy of the ion occurs at its thermochemical threshold, leading to an upper limit for $\Delta_f H^o_{298}(SF_4Cl^+)$ of 327 kJ mol^{-1}. Hence the value of $AE_{298,\ calc}(SF_4Cl^+)$ of 14.80 eV, column 6 of Table 1, is also an upper limit. It is therefore possible that E_{avail} has been underestimated, leading to lower values of $\langle f \rangle_T$ than those given in Table 2. The large values of $\langle f \rangle_T$, however, suggest that dissociation of the $\tilde{C}\ ^2E$ and $\tilde{D}\ ^2E$ states of SF_5Cl^+ to produce $SF_4Cl^+ + F$ is non-statistical, with relatively large amounts of the available energy being deposited into translation. If this is the case, then the true enthalpy of formation of SF_4Cl^+ at 298 K may be significantly lower than its upper limit value of 327 kJ mol^{-1}.

4.2. Electron impact excitation experiments

Fragment cations resulting from low-energy electron ionisation of SF_5Cl in the range 10–25 eV at a resolution of ca. 0.2 eV are shown in Figs. 4–6. The spectra have been normalised to variations in sample pressure and electron current. No allowance has been made for any mass discrimination effects of the quadrupole mass analyser, but the mass resolution was kept to the lowest possible value to minimise this problem. Thus, the values of the ion signals in these figures give a good indication of the relative cross-section for production of fragment ions. Some general comments are pertinent about these electron-induced experiments compared to the photon-induced coincidence studies (Section 4.1). In the electron ionisation experiment, the mass

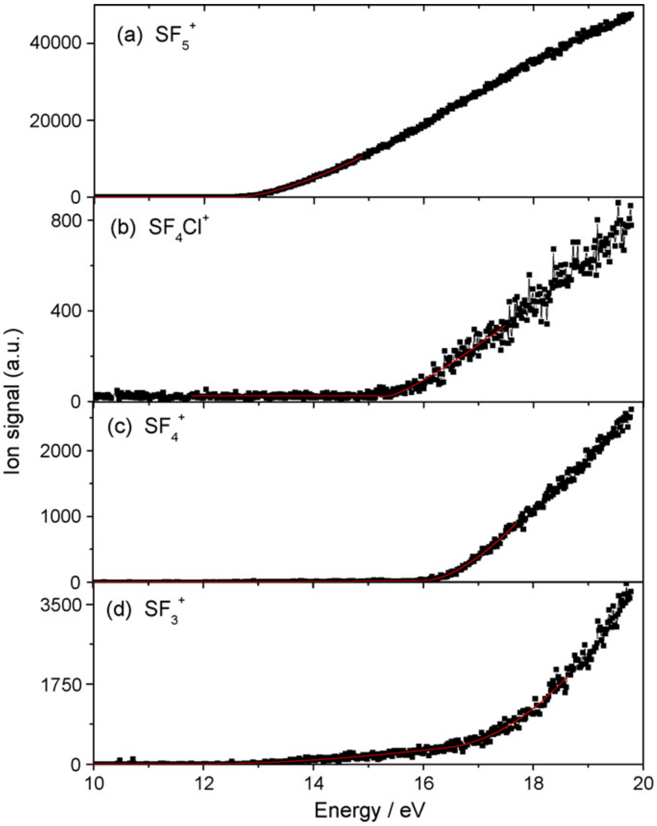

Fig. 4. Ionisation efficiency curves measured with an energy resolution of ca. 200 meV for production of (a) SF_5^+, (b) SF_4Cl^+, (c) SF_4^+ and (d) SF_3^+ by electron ionisation of SF_5Cl. The full curves are fits to the data to extract the corresponding EI threshold energies. The energy scale has been calibrated with argon, via its ionic $^2P_{3/2}$ threshold at 15.759 eV, measured under identical conditions.

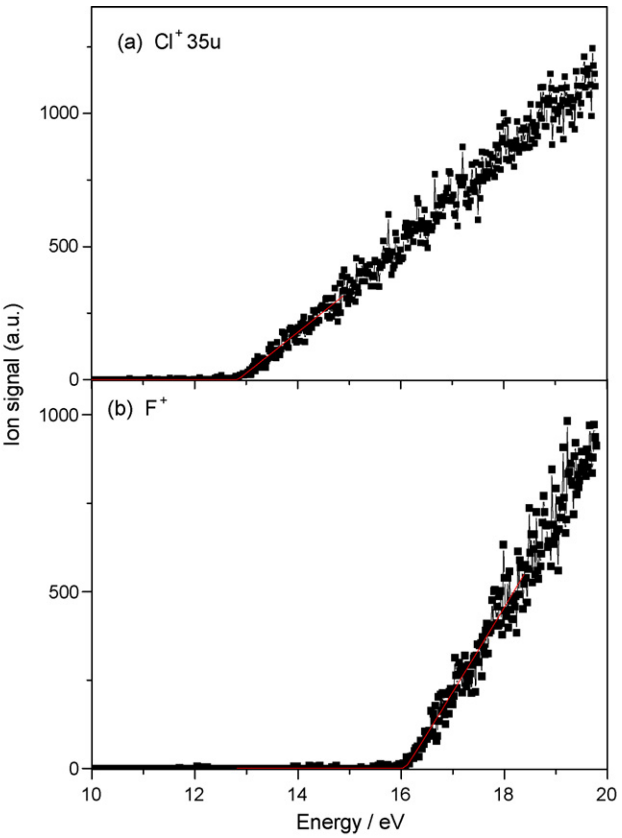

Fig. 5. Ionisation efficiency curves measured with an energy resolution of ca. 200 meV for production of (a) Cl^+ and (b) F^+ by electron ionisation of SF_5Cl. The full curves are fits to the data to extract the corresponding EI threshold energies. The accompanying fragment is assumed to be SF_5^- and SF_4Cl^-, respectively. The energy scale has been calibrated with argon, via its ionic $^2P_{3/2}$ threshold at 15.759 eV, measured under identical conditions.

and energy scales are unambiguous, and there is no equivalent to second-order effects in the photon experiments. Impurities, however, are potentially a serious problem since the quadrupole detects fragment ions whatever their source or method of production, and in addition a cation can be associated with production of either an electron or an anion; this experiment is therefore sensitive to ion-pair formation. By contrast, in the coincidence experiment using photons covering the same energy range as that of the electrons, the mass of the fragment cation is unambiguous, but because the cation is detected in coincidence with a photoelectron the experiment is not sensitive to ion-pair formation or gas impurities. Care must also be taken with the energy scale if second-order effects are significant for the dispersive diffraction grating in the beamline.

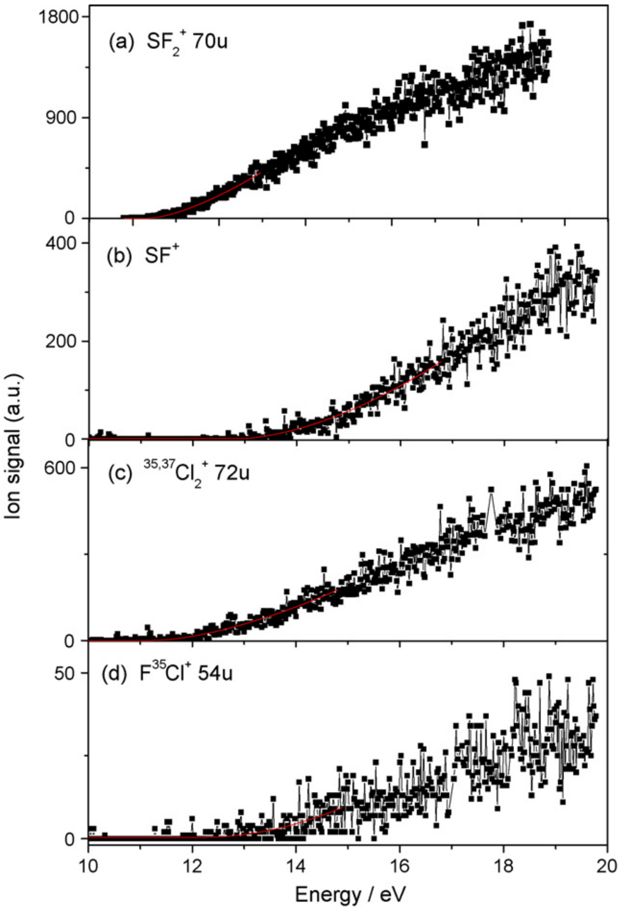

Fig. 6. Ionisation efficiency curves measured with an energy resolution of ca. 200 meV for production of (a) SF_2^+, (b) SF^+, (c) Cl_2^+ and (d) FCl^+ by electron ionisation of SF_5Cl. These ions arise from impurities in the gas sample. The full curves are fits to the data to extract the corresponding EI threshold energies. The energy scale has been calibrated with argon, via its ionic $^2P_{3/2}$ threshold at 15.759 eV, measured under identical conditions.

In these electron ionisation experiments, the cation is not detected in coincidence with another species. Thus, the experiments are not state-selected and the internal energy state of SF_5Cl is not defined following electron excitation. The only important quantity determined is the threshold energy of the fragment ion at the temperature of the experiment, ca. 298 K. As in the photon experiment (Section 4.1) the parent ion is not observed, ten fragment ions are now observed, and their threshold energies, as determined by the method described in Section 3, are given in column 3 of Table 1. The excitation functions for SF_5^+ and SF_4Cl^+ (Fig. 4) fit well to single-threshold functions, and their threshold energies are determined to be 12.65 ± 0.02 and 15.38 ± 0.09 eV, respectively. These values are significantly lower than those of the early work of Harland and Thynne (13.2 and 15.9 eV, respectively) [11], probably reflecting the improved sensitivity of this apparatus over earlier electron-ionisation spectrometers. However, they are greater than the AE_{298} values of these ions from photon-induced TPEPICO [this work] or PIMS spectroscopy [12], possibly reflecting the step function, and hence much steeper rise in cross-section at threshold for a photon-induced reaction. We can offer no explanation why the SF_4Cl^+ electron-induced threshold is ca. 0.6 eV greater than the photon-induced threshold, whereas for SF_5^+ the discrepancy is much smaller, ca. 0.3 eV. The excitation functions for SF_4^+ and SF_3^+ (Fig. 4) show curvature, and fit to double exponentials with thresholds of 12.0 ± 1.9 and 16.05 ± 0.05 eV for SF_4^+, 12.0 ± 0.6 and 16.5 ± 0.1 eV for SF_3^+, respectively. The lower-energy threshold has a much smaller weighting factor for both ions. The higher-energy thresholds are associated with production of SF_4^+ and SF_3^+ from SF_5Cl, and the values compare favourably with those from photon-induced experiments (Table 2). The lower-energy thresholds are associated with production of SF_4^+ and SF_3^+ from an impurity of SF_4 in the gas sample, the literature values for these AE values from SF_4 being 12.0 ± 0.3 and 12.6 ± 0.1 eV, respectively [26]. SF_4 was also detected as an impurity in the recent study of anions formed by low-energy electron attachment to SF_5Cl [4]. These lower-energy thresholds are not observed in the photon-induced experiment because ions are only detected here when they are in coincidence with a threshold photoelectron.

The signals from Cl^+ and F^+ are surprisingly strong (Fig. 5), and have single-value thresholds of 12.85 ± 0.05 and 16.08 ± 0.06 eV, respectively. These values are much higher than the calculated energy thresholds for $Cl^+ + SF_5 + e^-$ and $F^+ + SF_4Cl + e^-$ of 15.33 and 20.95 eV, respectively. Since the energy scale in these experiments is unambiguous, the only possibility is that Cl^+ and F^+ are formed with the associated anion SF_5^- and SF_4Cl^-, respectively. Since the electron affinity (EA) of the SF_5 radical is known, 3.80 eV [15], the energy threshold for production of $Cl^+ + SF_5^-$ can be calculated to be 11.53 eV which is 1.32 eV below the experimental threshold. The Cl^+ cation therefore may be formed at threshold translationally hot, with a maximum kinetic energy of $(127/162.5) \times 1.32 = 1.03$ eV. The EA of the SF_4Cl radical is unknown, but a similar calculation yields a lower limit of 4.88 eV; the error is difficult to quantify, but the dominant contributions will come from the enthalpy of formation of SF_4Cl and the error of 0.06 eV in the electron ionisation threshold value. At threshold, the F^+ cation will therefore have a translational kinetic energy between zero and $(143.5/162.5) \times [\mathrm{EA}(SF_4Cl) - 4.88]$ eV. The EA (SF_4Cl) value is very high for an electron affinity of a polyatomic free radical, with most species having values in the range ca. 0–4 eV [41]. However, calculations by Larkin and Schaefer at the MP2 level of theory with a variety of basis sets suggest that the vertical detachment energy of SF_4Cl lies in the range 4–6 eV[3]; the vertical detachment energy is defined as the vertical energy of the anion below that of the neutral where the neutral is frozen at the (optimised) C_{4v} geometry of the anion. Thus, using an aug-cc-pvtz basis set, they calculate the vertical detachment energy of SF_4Cl to be 5.74 eV, consistent with our lower limit experimental value of 4.88 eV. With this basis set, the vertical attachment energy (in which the anion is frozen at the energy of the (optimised) neutral molecule) is much less, 2.45 eV. In agreement with an earlier calculation of Gutsev and Ziegler [20], the structural calculation of Larkin and Schaefer predicts an increase in the S–Cl bond length of 0.016 nm, an increase in the S–F bond length of 0.012 nm, and a reduction in the FSCl bond angle of 8° upon addition of an extra electron to SF_4Cl.[3] Large values of an electron affinity can often accompany a significant change in geometry upon formation of an anion, conditions under which the vertical detachment and vertical attachment energies, on Franck–Condon grounds, are very different.

Fragment cations are also observed with much lower signal intensity at *m/e* values of 70, 51, 72, 74, 54 and 56 u. The spectra for ions with 70, 51, 72 and 54 u are shown in Fig. 6. The ratio of the signal strengths of the 72 u (Fig. 6c) and 74 u spectra are 6:1 at all energies above threshold, consistent with the peaks being due to $^{35,37}Cl_2$ and $^{37,37}Cl_2$. The 70 u spectrum is much stronger than 9/6 or 1.5 times the strength of the 72 u spectrum, so the former has contributions from both SF_2^+ and $^{35,35}Cl_2$; note that the 4% contribution of ^{34}S to all ion yields containing one sulfur atom is neglected. The SF_2^+ spectrum shown in Fig. 6(a) has had 1.5 times the 72 u spectrum subtracted for all energies, so it represents a 'pure' SF_2^+ ion yield. The SF^+ spectrum (Fig. 6b) at 51 u has no such ambiguity of assignment. The $F^{35}Cl^+$ spectrum (Fig. 6d) at 54 u has a very weak spectrum at 56 u due to $F^{37}Cl$ ca. three times weaker at all energies. All four ion yields fit well to single-threshold functions, with thresholds for SF_2^+, SF^+, Cl_2^+ and FCl^+ of 10.39 ± 0.16, 12.87 ± 0.25, 11.26 ± 0.26 and 12.17 ± 0.24 eV, respectively. The $Cl_2^+$and FCl^+ signals almost certainly arise from impurities of Cl_2 and FCl in the gas sample, with well-established ionisation energies from photoelectron spectroscopy of 11.48 and 12.66 eV [42,43]. The energetics of the SF_2^+ and SF^+ thresholds suggest that the source of these ions is also a gas-sample impurity of SF_2, since the ionisation energy of SF_2 and appearance energy of SF^+/SF_2 have been measured to be 10.08 and 13.9 ± 0.1 eV, respectively [44,45]. We are unable to explain the apparent presence of this impurity in the gas sample, given that the lifetime of SF_2 is believed to be only ca. 1 s.[4] Certainly, SF_2^+ and SF^+ cannot arise from dissociative electron ionisation of SF_5Cl since the lowest thresholds (e.g., $SF_2^+ + F_2 + FCl + e^-$) have calculated thresholds of at least 17 eV. Finally, we note that none of these four impurity ions are observed in the photon-induced coincidence study.

5. Conclusions

We have conducted a complementary study of the interaction of SF_5Cl in the gas phase with vacuum-UV photons (Daresbury, UK) and low-energy electrons (Innsbruck, Austria) from the onset of ionisation (ca. 12 eV) to 20 eV. The strengths and limitations of both techniques are contrasted and discussed. The photon-induced study has been performed under coincidence conditions in which the internal energy state of the initially-excited SF_5Cl is defined, whilst there is no state selectivity in the electron-induced study. The parent cation is not observed in either study, suggesting that its ground electronic state is repulsive following Franck–Condon vertical excitation. The fragment cations SF_5^+, SF_4Cl^+, SF_4^+ and SF_3^+ have been observed in both studies, with reasonable agreement in their threshold appearance energies. Using a variant of threshold photoelectron photoion coincidence spectroscopy applicable when the ground state of the parent cation is repulsive, we have determined the first dissociative ionisation energy of SF_5Cl to be 12.3 ± 0.2 eV, which leads to a value for the adiabatic ionisation energy for the SF_5 radical of 9.92 ± 0.28 eV. The electron-induced experiment is sensitive to ion-pair production, and we have observed the onsets for F^+ and Cl^+ production which are only possible energetically if the accompanying fragments are the anions SF_4Cl^- and SF_5^-.

---

[3] J. Larkin, H.F. Schaefer, private communication.

[4] C.A. de Lange, private communication.

The energetics are consistent with the literature value for the electron affinity of SF_5, and we determine a lower limit for the electron affinity of the SF_4Cl radical of 4.88 eV. This latter value is confirmed by preliminary ab initio calculations. The electron-induced experiment is very sensitive to gas impurities, and we can observe the effects of minute quantities of SF_4, FCl, Cl_2 and possibly SF_2 in the gas sample.

Acknowledgements

We thank Joe Larkin and Fritz Schaefer III for calculations on the EA (SF_4Cl) and useful discussions. We also thank Michael Parkes for running Gaussian 03 calculations on the molecular orbitals of SF_5Cl. The work was supported by EPSRC (GR/M/42794/01), by the Daresbury Laboratory, and by ESF short visit grants (EIPAM network). RYLC thanks the University of Birmingham for a Studentship.

References

[1] J.C. Creasey, H.M. Jones, D.M. Smith, R.P. Tuckett, P.A. Hatherly, K. Codling, Chem. Phys. 174 (1993) 441.
[2] For e.g., T.L. Williams, L.M. Babcock, N.G. Adams, Int. J. Mass Spectrom. 185–187 (1999) 759.
[3] G.K. Jarvis, R.A. Kennedy, C.A. Mayhew, R.P. Tuckett, J. Phys. Chem. A 104 (2000) 10766.
[4] M. Braun, M.W. Ruf, H. Hotop, P. Cicman, P. Scheier, T.D. Märk, E. Illenberger, R.P. Tuckett, C.A. Mayhew, Int. J. Mass Spectrom. 252 (2006) 234.
[5] R. Kewley, K.S.R. Murty, T.M. Sugden, Trans. Faraday Soc. 56 (1960) 1732.
[6] J. Bellet, R. Jurek, J. Chanussot, J. Mol. Spectrosc. 78 (1979) 16.
[7] C.J. Marsden, L.S. Bartell, Inorg. Chem. 15 (1976) 3005.
[8] R.R. Smardzewski, R.E. Noftle, W.B. Box, J. Mol. Spectrosc. 62 (1976) 449.
[9] R.L. DeKock, B.R. Higginson, D.R. Lloyd, Faraday Discuss. 54 (1972) 84.
[10] A.P. Klyagina, A.A. Levin, G.L. Gutsev, Chem. Phys. Lett. 77 (1981) 365.
[11] P. Harland, J.C.J. Thynne, J. Phys. Chem. 73 (1969) 4031.
[12] H. Baumgärtel, H.W. Jochims, E. Rühl, O. Losking, H. Willner, Z. Naturforsch. B 44 (1989) 21.
[13] B.M. Addison, K.H. Tan, G.M. Bancroft, F. Cerrina, Chem. Phys. Lett. 129 (1986) 468.
[14] C. Raynaud, S. Bodeur, J.L. Marechal, D. Bazin, P. Millie, I. Nenner, U. Rockland, H. Baumgärtel, Chem. Phys. 166 (1992) 411.
[15] M. Fenzlaff, R. Gerhard, E. Illenberger, J. Chem. Phys. 88 (1988) 149.
[16] K. Mitsuke, S. Suzuki, T. Imamura, I. Koyano, J. Chem. Phys. 93 (1990) 8717.
[17] C.A. Mayhew, A.D.J. Critchley, D.C. Howse, V. Mikhailov, M.A. Parkes, Eur. Phys. J. D 35 (2005) 307.
[18] C.A. Mayhew, A.D.J. Critchley, G.K. Jarvis, Int. J. Mass Spectrom. 233 (2004) 259.
[19] C. Atterbury, A.D.J. Critchley, R.A. Kennedy, C.A. Mayhew, R.P. Tuckett, Phys. Chem. Chem. Phys. 4 (2002) 2206.
[20] G.L. Gutsev, T. Ziegler, Inorg. Chem. 31 (1992) 1909.
[21] R.Y.L. Chim, R.A. Kennedy, R.P. Tuckett, W. Zhou, G.K. Jarvis, D.J. Collins, P.A. Hatherly, J. Phys. Chem. A 105 (2001) 8403.
[22] E.R. Fisher, B.L. Kickel, P.B. Armentrout, J. Chem. Phys. 97 (1992) 4859.
[23] P.A. Hatherly, D.M. Smith, R.P. Tuckett, Z. Phys. Chem. 195 (1996) 97.
[24] C.R. Howle, D.J. Collins, R.P. Tuckett, A.E.R. Malins, Phys. Chem. Chem. Phys. 7 (2005) 2287.
[25] V. Grill, H. Drexel, W. Sailer, M. Lezius, T.D. Märk, Int. J. Mass Spectrom. 205 (2001) 209.
[26] NIST Chemistry webbook, http://webbook.nist.gov/chemistry.
[27] R.L. Asher, B. Ruscic, J. Chem. Phys. 106 (1997) 210.
[28] J.C. Traeger, R.G. McLoughlin, J. Am. Chem. Soc. 103 (1981) 3647.
[29] V.A. Mikhailov, M.A. Parkes, R.P. Tuckett, C.A. Mayhew, J. Phys. Chem. A 110 (2006) 5760.
[30] M.A. Parkes, S. Ali, R.P. Tuckett, V.A. Mikhailov, C.A. Mayhew, Phys. Chem. Chem. Phys. 8 (2006) 3643.
[31] M.W. Chase, J. Phys. Chem. Ref. Data (1998) (monograph no. 9).
[32] C. Macho, R. Minkwitz, J. Rohmann, B. Steger, V. Wölfel, H. Oberhammer, Inorg. Chem. 25 (1986) 2828.
[33] S.G. Lias, J.E. Bartmess, J.F. Liebman, J.L. Holmes, R.D. Levin, W.G. Mallard, J. Phys. Chem. Ref. Data 17 (Suppl. 1) (1988).
[34] T.D. Märk, J. Chem. Phys. 63 (1975) 3731.
[35] G.E. Busch, K.R. Wilson, J. Chem. Phys. 56 (1972) 3626.
[36] I. Powis, P.I. Mansell, C.J. Danby, Int. J. Mass spectrom. Ion Phys. 32 (1979) 15.
[37] G.K. Jarvis, D.P. Seccombe, R.P. Tuckett, Chem. Phys. Lett. 315 (1999) 287.
[38] G.K. Jarvis, C.A. Mayhew, R.Y.L. Chim, R.A. Kennedy, R.P. Tuckett, Chem. Phys. Lett. 320 (2000) 104.
[39] H. Becker, J. Hrusak, H. Schwarz, D.K. Bohme, J. Chem. Phys. 100 (1994) 1759.
[40] C.E. Klots, J. Chem. Phys. 58 (1973) 5364.
[41] J.C. Rienstra-Kiracofe, G.S. Tschimper, H.F. Schaefer, S. Nandi, G.B. Ellison, Chem. Rev. 102 (2002) 231.
[42] H. van Lonkhuyzen, C.A. de Lange, Chem. Phys. 89 (1984) 313.
[43] R.L. de Kock, B.R. Higginson, D.R. Lloyd, A. Breeze, D.W.J. Cruickshank, D.R. Armstrong, Mol. Phys. 24 (1972) 1059.
[44] D.M. de Leeuw, R. Mooyman, C.A. de Lange, Chem. Phys. 34 (1978) 287.
[45] W. Gombler, A. Haas, H. Willner, Z. Anorg, Allg. Chem. 469 (1980) 135.